

1 *Caenorhabditis elegans* AF4/FMR2 family homolog *affl-2* is required for heat shock induced
2 gene expression

3

4 Sophie J. Walton^{*}, Han Wang^{*}, Porfirio Quintero-Cadena^{*}, Alex Bateman[†], and Paul W.
5 Sternberg^{*,1}

6 ^{*} Division of Biology and Biological Engineering, California Institute of Technology, Pasadena,
7 CA 91125.

8 [†] European Molecular Biology Laboratory, European Bioinformatics Institute, (EMBL-EBI),
9 Wellcome Genome Campus, Hinxton, Cambridge CB10 1SD, UK

10 ¹ Correspondence should be addressed to:

11 Paul W. Sternberg

12 Email: pws@caltech.edu

13 Phone: 626-395-2181

14 Address: Mail Code 156-29, 1200 E. California Blvd., California Institute of Technology,
15 Pasadena, CA 91125

16 Keywords: *affl-1*, *affl-2*, heat shock response, *C. elegans*, AF4/FMR2

17 Sophie J. Walton ORCID: 0000-0003-1320-1525

18 Han Wang ORCID: 0000-0002-1933-5762

19 Porfirio Quintero-Cadena ORCID: 0000-0003-0067-5844

20 Alex Bateman ORCID: 0000-0002-6982-4660

21 Paul W. Sternberg ORCID: 0000-0002-7699-0173

22

23 Running title: *affl-2* is essential for heat shock response

24 **Abstract**

25 To mitigate the deleterious effects of temperature increases on cellular organization and
26 proteotoxicity, organisms have developed mechanisms to respond to heat stress. In eukaryotes,
27 HSF1 is the master regulator of the heat shock transcriptional response, but the heat shock
28 response pathway is not yet fully understood. From a forward genetic screen for suppressors of
29 heat shock induced gene expression in *C. elegans*, we identified a new allele of *hsf-1* that alters
30 its DNA-binding domain, and three additional alleles of *sup-45*, a previously uncharacterized
31 genetic locus. We identified *sup-45* as one of the two hitherto unknown *C. elegans* orthologs of
32 the human AF4/FMR2 family proteins, which are involved in regulation of transcriptional
33 elongation rate. We thus renamed *sup-45* as *affl-2* (AF4/FMR2-Like). *affl-2* mutants are egg-
34 laying defective and dumpy, but worms lacking its sole paralog (*affl-1*) appear wild-type. AFFL-
35 2 is a broadly expressed nuclear protein, and nuclear localization of AFFL-2 is necessary for its
36 role in heat shock response. *affl-2* and its paralog are not essential for proper HSF-1 expression
37 and localization after heat shock, which suggests that *affl-2* may function downstream or parallel
38 of *hsf-1*. Our characterization of *affl-2* provides insights into the complex processes of
39 transcriptional elongation and regulating heat shock induced gene expression to protect against
40 heat stress.

41

42

43 **Introduction**

44 Heat is a universal source of stress in nature, which has detrimental effects including
45 disrupting cellular organization and upsetting proteostasis (Morimoto 1998). One way organisms
46 restore homeostasis after heat stress is through rapid transcriptional changes to upregulate genes
47 that assist with combating damaging effects of heat (Morimoto 1998; Hajdu-Cronin *et al.* 2004;
48 Richter *et al.* 2010). In eukaryotes, heat shock induced transcription is initiated when
49 transcription factors known as heat shock factors (HSFs) are activated and bind to heat shock
50 elements (HSEs) in promoters (Morimoto 1998), and HSF1 has been identified as the primary
51 regulator of heat shock induced transcription in eukaryotes (Åkerfelt *et al.* 2010; Richter *et al.*
52 2010). The current model for transcriptional control of heat shock response by HSF1 is as
53 follows: under normal conditions chaperones sequester HSF1 and upon heat stress the
54 chaperones disassociate with HSF1 so HSF1 is free to upregulate other genes (Richter *et al.*
55 2010; Voellmy and Boellmann 2007). However, the complete regulatory system that is
56 responsible for the precise transcriptional control of heat shock response is not yet fully
57 understood (Richter *et al.* 2010).

58 Although regulation of initiation in heat shock induced transcription has been well
59 characterized, it is known that transcription is also tightly regulated at the elongation and
60 termination steps (Kuras and Struhl 1999; Sims *et al.* 2004; Saunders *et al.* 2006; Lenasi and
61 Barboric 2010). For some genes involved in development and stress, RNA Polymerase II
62 becomes paused at the promoter-proximal region, and escape from the paused state becomes a
63 rate limiting process in transcription (Levine 2011; Lin *et al.* 2011; Zhou *et al.* 2012; Luo *et al.*
64 2012a) In metazoans, Positive Transcription Elongation Factor beta (P-TEFb), a heterodimeric

65 kinase complex composed of CDK-9 and a Cyclin T1 Partner, causes RNA Polymerase II and
66 associated factors to become phosphorylated to stimulate promoter escape (Levine 2011; Zhou
67 *et al.* 2012; Luo *et al.* 2012b). When performing this function, P-TEFb participates in the super
68 elongation complex (SEC): a multi-subunit complex composed of a P-TEFb, an AF4/FMR
69 family protein (AFF1 or AFF4), a Pol II elongation factor (ELL, ELL2 or ELL3), a partner
70 protein (EAF1 or EAF2), and an ENL family protein (ENL or AF9) (Lin *et al.* 2010; Luo *et al.*
71 2012b). Although both AFF4 and AFF1 serve as scaffolds in the SEC, they have been found to
72 work in different processes; e.g., AFF4 has been found to be more important for HSP70
73 transcription and AFF1 has been linked to promoting HIV transcription (Lu *et al.* 2015).

74 *Caenorhabditis elegans* has been used as a multicellular *in vivo* model to perform genetic
75 analysis of homologs of components of the SEC. The *C. elegans* homolog of the ELL gene
76 family (*ell-1*) and its partner (*eaf-1*) are necessary for embryonic development and heat shock
77 induced transcription (Cai *et al.* 2011). In addition, *cdk-9*, *cit-1.1*, and *cit-1.2*, homologs of
78 CDK9 and cyclin T1, are necessary for phosphorylation of Ser2 in RNA polymerase II in the
79 soma (Shim *et al.* 2002; Bowman *et al.* 2013). However, a *C. elegans* version of the AF4/FMR2
80 family proteins, which serve as the scaffolds for the SEC, has not yet been identified.

81 In a genetic screen for suppressors of heat shock induced gene expression, we identified a
82 new reduction of function *hsf-1* allele and cloned a *C. elegans* AF4/FMR2 homolog, *affl-2*
83 (AF4/FMR2-Like). *affl-2* encodes a previously uncharacterized protein that is predicted to have
84 two nuclear localization signals and a collection of disordered residues at its N terminus. Indeed,
85 AFFL-2 is a broadly expressed nuclear protein, and its nuclear localization is necessary for its
86 role in heat shock response. In addition to being defective in heat shock response, *affl-2* mutants

87 are dumpy, egg-laying defective, and some have protruding intestines from their vulvas. *affl-2* is
88 not necessary for the proper localization and expression of HSF-1 pre or post heat shock,
89 suggesting that *affl-2* may function downstream of *hsf-1*. Our identification and characterization
90 of *affl-2* furthers our understanding of heat shock response induced transcriptional regulation in
91 *C. elegans* and validates the power of *C. elegans* for genetic analysis of general transcriptional
92 control.
93

94 **Materials and Methods**

95 ***C. elegans* cultivation**

96 *C. elegans* were grown using the methods described in (Brenner 1974). Strains were
97 maintained on NGM agar plates at room temperature (20 °C) and fed OP50, a slow-growing
98 strain of *Escherichia coli*. A list of strains used in this study can be found in Supplementary
99 Experimental Procedures.

100 **Genomic Editing**

101 We made *affl-1* mutants by inserting the STOP-IN cassette in the 5' end of the coding
102 sequence of *affl-1* using CRISPR/Cas9 with a co-conversion marker (Wang *et al.* 2018). We
103 injected N2 worms to create *affl-1* (*sy1202*) single mutants, and we injected *affl-2*(*sy975*) worms
104 to create *affl-2*(*sy975*) *affl-1*(*sy1220*) double mutants. *sy1202* and *sy1220* had the same molecular
105 change in the *affl-1* gene. The sequence change is a 43bp insertion with 3-frame stop codon and
106 is near the 5' end of the gene *Y55B1BR.1/affl-1*:

107 5' flanking seq: CCGTACCCGTAGAATGCTTGAAGAAATGGCCGGCC
108 Insertion: GGGAAAGTTTGTCCAGAGCAGAGGTGACTAAGTGATAA
109 3' flanking seq: TCGTGGGAACTAAACCATTGAGCCAGCTTCCTCGAAG

110
111 Primers for genotyping and sequencing can be found in the Supplementary Experimental
112 Procedures.

113 **Generation of Transgenic Lines**

114 Methods to generate transgenic animals were adapted from Mello and Fire (1995). The
115 *affl-2* driver strain was constructed by injecting 25 ng/μl of pSJW003 along with 40 ng/μl of
116 *Punc-122::rfp* and 35 ng/μl of 1 kb DNA ladder (NEB) into the GFP effector strain *syIs300*, and
117 then outcrossing the resulting worms to add the GFP::H2B effector strain *syIs407* in place of
118 *syIs300* (Wang *et al.* 2017). All *affl-2* rescue variants were constructed by injecting 10 ng/μL of

119 the plasmid containing the rescue construct along with 80 ng/ μ l of pBluescript and 10 ng/ μ L of
120 the co-injection marker plasmid KP1368(*Pmyo-2::nls::mCherry*) into the strain PS8082 (*syIs231*
121 *II; affl-2 (sy975) III*). A list of transgenic lines and plasmids used can be found in the
122 Supplementary Experimental Procedures.

123 ***lin-3c* overexpression assays**

124 We used pumping quiescence as a readout for expression of heat shock driven *lin-3c*, for
125 cessation of pumping is characteristic of *lin-3c* overexpression induced quiescence. We adapted
126 our *lin-3c* overexpression assay from Van Buskirk and Sternberg (2007). 15-30 L4 animals were
127 picked onto NGM agar plates that were seeded 48-72 hours prior. 16-20 hours later, plates with
128 adult animals were parafilm and placed in a 33 °C water bath for 15 minutes. We used a 15-
129 minute heat shock rather than a 30-minute heat shock because we wanted to be able to detect
130 weaker suppressors. Plates were then left in 20 °C with their lids open to recover for 3 hours
131 before scoring for pumping quiescence. By this time, all worms would have recovered from the
132 mild heat shock and would thus exhibit only *lin-3c* overexpression dependent quiescence.
133 Pumping quiescence was scored using a stereomicroscope on 25-50x magnification, and
134 quiescence was defined as a cessation of movement of the pharyngeal bulb.

135 **Isolation of suppressors**

136 EMS Mutagenesis

137 Mutagenesis was performed on about 500 late L4 hermaphrodites (PS7244) as described
138 by Brenner (1974). In particular, worms were incubated in a solution of 4 mL M9 with 20 μ L
139 EMS (Sigma) for 4 hours. At the end of the 4 hours, we washed the worms three times each with
140 3 mL of M9 to dilute the EMS. We then plated the mutagenized worms on a seeded NGM agar

141 plate outside the OP50 lawn and left them to recover for at least 30 minutes before plating the P0
142 worms.

143 To screen a synchronized F2 population, we treated the F1 adults with alkaline
144 hypochlorite (bleach) treatment to isolate the eggs of the F2 generation (Protocol B from Porta-
145 de-la-Riva *et al.* 2012). After bleaching treatment, we immediately plated the F2 generation
146 eggs. These steps ensured that all of our F2 animals reached adulthood at roughly the same time.

147 We performed the *lin-3c* overexpression assay as described above on adult F2 worms.
148 We isolated worms who did not exhibit pumping quiescence onto separate plates, and we
149 screened their progeny (F3 generation) to ensure that the phenotype was stable. Mutants isolated
150 from different P₀ plates were deemed independent.

151 Complementation Testing with *hsf-1* and *affl-2* Mutants

152 To identify *hsf-1* and *affl-2* mutants, we performed complementation testing with *hsf-*
153 *1(sy441)*, *affl-2(sy509)*, and *affl-2(sy978)* mutants. Note that *affl-2* was originally named *sup-45*.
154 *hsf-1(sy441)*, *affl-2(sy509)*, or *affl-2(sy978)* hermaphrodites were crossed with *syIs197* males.
155 We crossed the resultant male cross progeny into suppressors, and we performed the *lin-3c*
156 overexpression assay on F1 cross progeny of the cross to assay complementation.

157 SNP Mapping

158 We used the polymorphic Hawaiian strain CB4856 to perform SNP mapping of our
159 suppressor loci (Doitsidou *et al.* 2010). Our SNP mapping strain was PS7421, which we created
160 by outcrossing PS7244 ten times to CB4856. We followed the Hobert's Lab protocol for worm
161 genomic DNA for SNP Mapping (pooled samples) (Oliver Hobert Lab) to prepare genomic
162 DNA from the progeny of 50 suppressors and 50 non suppressors crossed with PS7421. For
163 identifying *Y55B1BR.2* we sequenced PS75971 (*syIs231 II*; *affl-2(sy978) III*) crossed into

164 PS7421 and we sequenced PS8082 (*syIs231 II*; *affl-2 (sy975) III*) in a N2 background. We
165 analyzed our sequencing results using MiModD mapping software to identify putative mutations
166 (Maier *et al.* 2014).

167 **Protein Sequence Analysis**

168 Y55B1BR.2 similarity to AF4 was found in the first iteration of a JackHMMER iterative
169 search on the EMBL-EBI webserver (Potter *et al.* 2018). Further rounds of searching revealed
170 homologues in a wide range of eukaryotic species. The search was performed against Reference
171 Proteomes using the phmmer algorithm with the following settings:

172 **HMMER Options:** -E 1 --domE 1 --incE 0.01 --incdomE 0.03 --mx BLOSUM62 --pextend 0.4
173 --popen 0.02 --seqdb uniprotrefprot
174

175 We used the MUSCLE alignment tool with the default settings to create multiple
176 sequence alignments (Edgar 2004). To determine the location of the predicted NLSs we used the
177 cNLS mapper with a cut-off score of 0.5 and the option to search for bipartite NLSs with a long
178 linker within terminal 60-amino acid regions (Kosugi *et al.* 2008, 2009a; b). We checked that
179 these predictions were consistent with PSORT and NucPred. We used IUPred2A long disorder
180 (Dosztányi *et al.* 2005; Dosztanyi *et al.* 2018) to predict disordered regions of AFFL-2, AFFL-1,
181 AFF1, and AFF4. We used ANCHOR2 software to predict the presence of the disordered protein
182 binding regions of AFFL-2, AFFL-1, AFF1, and AFF4 (Dosztányi *et al.* 2009; Dosztanyi *et al.*
183 2018). The alignment of the C-terminal homology domain (CHD) was generated using the
184 MUSCLE alignment tool on a selected set of 16 eukaryotic homologues identified using
185 Jackhmmmer (Edgar 2004).

186 **Molecular Biology**

187 We used Roche Taq for genotyping PCR products < 1 kb, and we used NEB Phusion
188 High Fidelity or NEB High Fidelity Q5 for PCR of all cloning inserts and genotyping PCR
189 products that were > 1kb. NEB T4 Ligase was used to construct pSJW003. The NEBuilder HiFi
190 DNA Assembly Master Mix was used for Gibson Assembly of pSJW005, pSJW035, pSJW036,
191 pSJW040, and pSJW041. We used DH5 α competent cells for all transformation, and we plated
192 all transformed cells on carbenicillin LB plates. A detailed list of oligos and plasmids can be
193 found in the Supplementary Experimental Procedures.

194 **Microscopy**

195 For images of plate phenotypes, one day old adult worms were filmed on plates seeded
196 within 24 hours after the L4 larvae stage. We used a Wild Makroskop M420 dissecting scope at
197 32x or 40x magnification.

198 Images of *affl-2* expression and localization of HSF-1::GFP and AFFL-2::GFP were
199 taken using a Plan Apochromat 10x or 63x/1.4 Oil DIC objective in a Zeiss Imager Z2
200 microscope with an Axiocam 506 Mono camera using ZEN Blue 2.3 software. Young adults
201 were used for imaging, because their lower fat content made it easier to detect fluorescent
202 proteins. Worms were anesthetized in 3 mM levamisole and mounted on 2 % agarose pads. Z-
203 stacks were taken at 63x and maximum-intensity projections were generated using Fiji/ImageJ
204 software (Schindelin *et al.* 2012). Z-stacks were used for images of HSF-1::GFP localization,
205 and when indicated for AFFL-2::GFP localization.

206 Our method to image HSF-1::GFP was adapted from Morton and Lamitina (2013). To
207 image HSF-1::GFP after heat shock, worms were mounted on slides and incubated in a preheated
208 PCR machine at 35 °C for five minutes. The lid of the PCR machine was left open, for it did not
209 reach 35 °C. Instead, slides were placed in a foil packet on top of the PCR wells. We found that a

210 five-minute heat shock was long enough to cause worms to form granules consistently and
211 longer incubation caused the plates to dry out. Worms were imaged immediately after heat
212 shock. Non heat shock controls were left on the benchtop (20 °C) for five minutes prior to
213 imaging. In our image analysis, we selected nuclei manually, and chosen nuclei were segmented
214 automatically. We detected granules in chosen nuclei automatically using the blob detector
215 function from scikit-image (Walt *et al.* 2014). We used the mean intensity of the segmented
216 nuclei and granules after background subtraction to determine HSF-1::GFP nuclear intensity.

217 To image AFFL-2::GFP after heat shock, worms were heat shocked following the same
218 protocol as we used for the *lin-3c* overexpression assay. We choose to use this protocol rather
219 than the one adapted from (Morton and Lamitina 2013) because we wanted to recreate the
220 conditions of the worms were in during the genetic screen. After the heat shock worms were
221 immediately mounted onto slides and imaged.

222 **Data Analysis**

223 Unless otherwise specified, data analysis was carried out using Python 3.7 with standard
224 scientific libraries (Jones *et al.* 2001) and version 0.041 of the bebi103 package (Bois 2018).

225 Determining pumping quiescence frequency

226 We used a Bayesian modeling framework to estimate the frequency of worms pumping
227 after heat shock in the *lin-3c* overexpression assay (Bois 2018)

228 Our prior distribution for ϕ was:

$$\phi \sim \text{Beta}(\alpha, \beta)$$

229 Where, α, β are parameters for the Beta distribution that we specified. Our likelihood for n , the
230 number of worms exhibiting pumping quiescence was

$$n \sim \text{Binomial}(N, \phi)$$

231 where N is the number of worms in each experiment, n is the number pumping, and ϕ is the
232 probability of pumping. We used Stan to sample from the posterior distribution and find
233 confidence intervals for the parameter estimates (Stan Development Team, 2018).

234 Quantification of HSF-1 Expression and Nuclear Granule Formation

235 We used non-parametric bootstrapping to estimate the mean of HSF-1 nuclear intensity
236 before heat shock, HSF-1 granule intensity after heat shock, and estimate of the mean of the
237 number of granules per nuclei formed in each strain. We used the permutation test to compute all
238 reported p-values, for we did not have a good parametric model to explain the data generating
239 processes.

240

241 **Results**

242 **A genetic screen of pumping quiescence suppression yields new alleles involved in heat** 243 **shock transcription response**

244 To identify genes involved in heat shock response, we conducted a forward genetic
245 screen to search for suppressors of pumping quiescence caused through *Phsp-16.41* (promoter of
246 *hsp-16.41*) driven *lin-3* (Fig 1A). When overexpressed in adult animals, *lin-3*, encoding the *C.*
247 *elegans* ortholog of the epidermal growth factor (EGF), causes a reversible state of quiescence
248 that is characterized by cessation of feeding, locomotion, defecation, and decreased
249 responsiveness (Van Buskirk and Sternberg 2007). *hsp-16.41*'s expression is induced by heat
250 shock; therefore, placing *lin-3* under the control of *Phsp-16.41* gives us temporal control of
251 quiescence. We screened for animals which are defective in downstream steps of quiescence or
252 do not express the transgene properly by searching for pumping animals after heat shock (Fig
253 1A). We expected that some suppressors would be defective in heat shock induced transcription

254 of the *lin-3* transgene. Indeed, we found that one of the strong suppressors, *sy1198*, is recessive
255 and was mapped to the chromosome I (data not shown). The gene *hsf-1* is also located on
256 chromosome I, and it was identified from a similar screen using a transgene with a gain-of-
257 function *goa-1* driven by the promoter of *hsp-16.2*, another heat shock response gene similar to
258 *hsp-16.41* (Hadju-Cronin et. al, 2004). We found that *sy1198* and *hsf-1(sy441)* failed to
259 complement for suppression of quiescence, which indicated that *sy1198* is an allele of *hsf-1*. By
260 Sanger sequencing, we found *sy1198* is a T to A mutation in the *hsf-1* gene, which leads to a
261 Leucine to Glutamine substitution (L93Q) in the predicted DNA binding domain of HSF-1
262 protein (Table 1, Fig 1b; Hadju-Cronin *et al.* 2004). As null mutants of *hsf-1* are lethal (Li *et al.*
263 2016), *sy1198* is likely to be a weak loss-of-function allele.

264

265 **AFFL-1 and AFFL-2 are homologs of members of the AF4/FMR2 family**

266 We used Hawaiian SNP mapping and whole genome sequencing to find candidates for
267 causal mutations of the suppression of quiescence. We noticed that a group of suppressors which
268 failed to complement one another had mutations in the uncharacterized gene *Y55B1BR.2*, and
269 their mapping position (Fig S1) was similar to that of *sup-45*. Hadju-Cronin *et al.* identified *sup-*
270 *45* mutants that are defective in heat shock induced transgene expression, but they were unable to
271 clone the gene. We found that our *Y55B1BR.2* mutants failed to complement *sup-45(sy509)*,
272 which confirmed that the suppressors are alleles of *sup-45*. We determined the molecular
273 changes of our three *sup-45* alleles and two previously described *sup-45* using Sanger
274 sequencing, and indeed all had mutations in *Y55B1BR.2* (Table 1). For the rest of our
275 experiments, we used *sy975*, which contains a nonsense mutation at residue 456 (Fig 1C-D,
276 Table 1).

277 We found that Y55B1BR.2 is predicted to have two nuclear localization signals (NLS),
278 which suggested that it is a nuclear protein (see Methods). Additionally, Y55B1BR.2 has an
279 adjacent paralog *Y55B1BR.1*, whose encoding gene's start codon is separated from the stop
280 codon of *Y55B1BR.2* by only 489 nucleotides ("Y55B1BR.2 (gene) - WormBase: Nematode
281 Information Resource). Using JackHMMER (Potter *et al.* 2018), we found that Y55B1BR.2 and
282 Y55B1BR.1 are homologs of AFF4, which is a member of the human AF4/FMR2 family. Based
283 this homology we chose to name *Y55B1BR.1* as *affl-1* (AF4/FMR2 Like) and *Y55B1BR.2* as *affl-*
284 2. The AF4/FMR2 family includes the proteins AFF4 and AFF1, which serve as scaffold
285 proteins for multi-subunit super elongation complexes (SECs) that assist with releasing RNA
286 polymerase from promoter-proximal pausing (He and Zhou 2011; Lu *et al.* 2014; Mück *et al.*
287 2016. AFF1 and AFF4 both consist of an intrinsically disordered N-terminus that interacts with
288 other members of the SEC and a C-terminal homology domain (CHD) that is conserved among
289 members of the AF4/FMR2 family (Chen and Cramer 2019). AFF4's binding sites to SEC
290 partners have been studied and are diagramed in Fig 2B. Similarly, AFFL-2 is also predicted to
291 have disordered residues, most of which are in its N-terminus (Fig 2A). Disordered proteins
292 sometimes have protein binding domains that are disordered in isolation but become structured
293 upon binding (Dosztányi *et al.* 2009), and AFFL-2 has three such predicted disordered protein
294 binding regions in its N-terminus (Fig 2A).

295 Multiple Sequence Alignment of *H. sapiens* AFF1 and AFF4 along with *C. elegans*
296 AFFL-2 and AFFL-1 reveals that most of the similarity between the four proteins is in the
297 conserved C-terminal Homology Domain (CHD) of the AF4/FMR2 family members (Fig 2C,
298 Fig S2). The CHD of AFF4 has been shown to bind nucleic acids, form homodimers, and form
299 heterodimers with the AFF1-CHD *in vitro* (Chen and Cramer 2019). Interestingly, our sequence

300 searches identified previously unknown homologues of AF4/FMR2 proteins in *Arabidopsis*
301 *thaliana*, *Dictostelium discoideum*, *Acanthamoeba castellani* and sporadic yeast species.
302 Gopalan and colleagues previously identified a homologue within *Schizosaccharomyces pombe*
303 (Gopalan *et al.* 2018).

304

305 ***affl-2* mutants, but not *affl-1* mutants, are Egl, Dpy, and deficient in heat shock response**

306 *affl-2* mutants have been found to be Egl (EGg Laying defect), Dpy (Dumpy) and
307 deficient in heat shock induced transcription (Hajdu-Cronin *et al.* 2004). We also noticed that
308 some *affl-2* mutants have their intestines protruding from their vulvas (Fig 1E). We did not
309 observe such hernias in either *hsf-1(sy441)* or *hsf-1(sy1198)* worms.

310 We did not find any *affl-1*—the paralog of *affl-2*— mutants in our screen, so we made a
311 null mutant of *affl-1* to see if it is also necessary for heat shock induced gene expression. *affl-1*
312 mutants appear wild-type and do not have any of the morphological phenotypes characteristic of
313 *affl-2* mutants (Fig 1E). We also made *affl-2(sy975) affl-1(sy1220)* double-mutant animals,
314 which we found are Dpy, Egl, and have herniated intestines. We did not notice any obvious
315 defects in the double mutants that are not present in *affl-2(sy975)* single mutants (Fig 1E).

316 *affl-2* has been identified in two independent forward genetic screens using different
317 transgenes: one driven by *Phsp-16.2* (where it was called *sup-45*) and the other by *Phsp-16.41*. It
318 has already been demonstrated that *hsp-16.2* transcription is eliminated in *hsf-1* and *affl-2*
319 mutants worms using qPCR (Hajdu-Cronin *et al.* 2004). Since *hsp-16.2* and *hsp-16.41* share the
320 same regulatory sequence and are both induced by heat shock (Jones *et al.* 1986), we believe that
321 *hsp-16.41* transcription is also likely eliminated in *hsf-1* and *affl-2* mutants. Thus, we decided to
322 use heat shock inducible pumping quiescence, due to expression of *Phsp-16.41*, driven *lin-3* as a

323 readout for *hsp-16.41* expression. We estimated ϕ , the probability of a given worm pumping
324 after heat shock, to see whether the *hsp-16.41* promoter is active under heat shock conditions in
325 *affl-2*, *hsf-1*, *affl-1*, and *affl-2 affl-1* mutants (Fig 1F). We also ensured that all mutants pump at
326 wild type levels prior to heat shock (Fig 1F). The estimates of ϕ for *hsp-16.41:lin-3c* and *affl-*
327 *1(sy1202); hsp-16.41:lin-3c* were both 0, which indicates that there are no defects in heat shock
328 induced *hsp-16.41* expression. The estimates of ϕ for wild type, *Phsp-16.41:lin-3c; affl-*
329 *2(sy975)*, *Phsp-16.41:lin-3c; hsf-1(sy441)*, *Phsp-16.41:lin-3c; hsf-1(sy1198)*, *Phsp-16.41: affl-*
330 *2(sy975) affl-1(sy1220)* were all close to one, which indicates that these mutants were not
331 expressing the *lin-3c* transgene after heat shock. These results confirmed that *hsf-1* and *affl-2*, but
332 not *affl-1*, are necessary for heat shock induced *hsp-16.41* expression.

333

334 **AFFL-2 is a broadly expressed nuclear protein**

335 We cloned the first 3 kb of sequence upstream from *affl-2*'s start codon as *affl-2*'s 5'
336 regulatory region and promoter. We used this sequence to create a cGAL driver (Wang et al.
337 2017), which we crossed with a GFP::*H2B* effector to create a transcriptional reporter for *affl-2*.
338 GFP was visible in all tissues in worms of all stages, which indicates that *affl-2* is ubiquitously
339 expressed (Fig 3A). To observe the subcellular localization of AFFL-2, we used our cloned *affl-2*
340 promoter to drive AFFL-2 cDNA::*GFP*. *affl-2(sy975)* mutants with the transgene appear wild-
341 type and are able to express the *hsp-16.41* promoter driven *lin-3c* transgene (Fig 3E). Therefore,
342 we believe that our fusion protein is functional, and our cloned promoter for *affl-2* reflects its
343 endogenous expression pattern. AFFL-2::*GFP* is exclusively located in the nucleus prior to heat
344 shock, and we do not see any noticeable difference in AFFL-2::*GFP* localization or intensity
345 between worms before and after heat shock (Fig 3B).

346 As shown previously, *affl-1* is not necessary for heat shock induced *hsp-16.41*
347 transcription despite also being a homolog of AFF1 and AFF4 (Fig 1E). Additionally, our
348 Multiple Sequence Alignment suggests that AFFL1 shares little similarity with the first 135
349 amino acids of AFFL2, and AFFL-1 is not predicted to have any NLS (Fig 2, see Methods). We
350 thus decided to investigate the role of AFFL-2's N-terminus, which contains its predicted NLSs
351 and the majority of its predicted disordered residues (Fig 1D, 2A) by creating alternative
352 versions of AFFL-2 with modified N termini (Fig 3C). First, we created a modified AFFL-
353 2::GFP in which we removed 129 amino acids from the N terminus of AFFL-2. This
354 modification eliminated both predicted NLSs and the majority of the disordered residues. To test
355 the necessity of the disordered residues independently from the NLS, we created a construct in
356 which we substituted the deleted residues with the SV40 NLS. To test the role of the disordered
357 nature of the domain independently of its sequence, we made another construct that included the
358 artificial NLS and the 212 residue fused in sarcoma low complexity (FUS LC) domain. FUS is
359 one of three RNA binding proteins with LC domains that when fused to DNA binding domains
360 cause a variety of cancers (Arvand and Denny 2001; Guipaud *et al.* 2006; Lessnick and Ladanyi
361 2012). 84 % of the FUS LC domain consists of glycine, serine, glutamine, and tyrosine, and at
362 high concentrations the domain has been shown to polymerize. Kwon *et al.* (2013) also
363 demonstrated that the FUS LC domain fused to the GAL4 DNA binding domain can induce
364 transcriptional activation. As a control, we added a similar region but with 10 tyrosines mutated
365 to serines, which was shown to prevent the GAL4 and FUS LC fusion transcriptional activation
366 abilities (Kwon *et al.* 2013).

367 We found that in a wild-type background, all of the altered AFFL-2 proteins containing
368 an NLS are observed in the nucleus (Fig 3D). The modified AFFL-2 lacking the artificial NLS is

369 primarily located in the nucleus, but we saw that some of the protein is present in the cytoplasm
370 (Fig 3D, Fig S3). To test whether the nuclear localization of this construct is dependent on the
371 presence of wild type AFFL-2, we introduced the modified AFFL-2 with N-terminal deletion in
372 *affl-2(sy975)* animals. The localization of AFFL-2::N-terminal Deletion::GFP was similar in
373 both a wild type and *affl-2(sy975)* background: some animals had it strictly localized to the
374 nucleus while others had it in the cytoplasm as well (Fig S3). We did not expect this modified
375 protein to localize to the nucleus, but this result suggests there is an alternative mechanism for its
376 nuclear import. Introducing the modified AFFL-2 with the deletion, but no other alterations, did
377 not rescue any morphological defects of *affl-2(sy975)* worms (Fig S4). However, the constructs
378 with an artificial NLS rescued the morphological defects of *affl-2(sy975)* mutants (Fig S4).

379 To determine the extent that the constructs rescued the heat shock induced gene expression
380 defects of *affl-2(sy975)*, we estimated the probability of worms exhibiting pumping quiescence
381 due to heat shock induced *Phsp-16.41: lin-3c* expression (Fig 3E). The estimate of ϕ (the
382 probability of pumping after heat shock) for *affl-2(sy975)* animals with a wild type copy of
383 AFFL-2::GFP was $0_{0,0}^{0,0}$ (estimated mean with lower and upper subscripts denoting lower and
384 upper bounds for estimated 95% confidence interval), which demonstrates that the full AFFL-
385 2::GFP construct is functional. The estimates for ϕ for the deletion-only construct and the
386 construct with the addition of the modified FUS LC domain were both relatively high
387 ($0.511_{0,477}^{0,526}$, $0.406_{0,365}^{0,416}$), and the estimates for ϕ for constructs with only the artificial NLS and
388 the FUS LC were much lower ($0.157_{0,131}^{0,163}$ and $0.166_{0,148}^{0,173}$, respectively). Even though the
389 modified AFFL-2 with both predicted NLSs removed can be seen in the nucleus, adding back the
390 artificial NLS significantly increased the performance of AFFL-2. This suggests that exclusive
391 restriction of AFFL-2 in the nucleus is important for its function in heat shock response. Adding

392 back the low complexity FUS LC did not further increase the performance of the modified
393 AFFL-2, but the modified (Tyrosine to Serine) FUS LC hindered the performance of AFFL-2. It
394 is believed that FUS increases transcriptional activity by enhancing recruitment of RNA
395 polymerase II, for mutants that bind RNA polymerase II better increase transcription (Kwon *et*
396 *al.* 2013), and thus this result suggests that the role of AFFL-2 is not to enhance recruitment of
397 RNA polymerase

398 ***affl-1* and *affl-2* do not significantly influence HSF-1 localization and expression**

399 Since *hsf-1* is an essential gene, we could not perform traditional epistasis experiments
400 using the null mutants to determine whether, and if so how, *affl-2* and *hsf-1* genetically interact.
401 Instead, we used an *hsf-1* translational reporter to determine if *affl-2* and/or *affl-2* are necessary
402 for proper localization and expression of HSF-1. *C. elegans* HSF-1 is a ubiquitously expressed
403 nuclear protein, and HSF-1 will aggregate to form nuclear stress granules after heat shock
404 (Morton and Lamitina 2013). The HSF-1 foci do align with marks of active transcription and are
405 dependent on the HSF1 DNA binding domain, but the putative sites of the foci are still unknown
406 (Morton and Lamitina 2013). We quantified the formation of granules after heat shock using the
407 *P_{hsf-1}::HSF-1::GFP* transgene from Morton and Lamitina (2013) (Fig 4). We also quantified the
408 intensity of the granules after heat shock and the intensity of HSF1::GFP prior to heat shock for
409 all genotypes (Fig S5). We found that HSF-1 expression prior to heat shock is similar in all
410 genotypes (Fig S5a), which demonstrates that neither *affl-2* nor *affl-1* are critical for regulating
411 HSF1 expression. Although some differences of means of the number of granules (Fig 4b) and
412 intensity (Fig S5b) of HSF-1::GFP between genotypes are statistically significant ($p < 0.05$),
413 there is still too much overlap between the different distributions of HSF-1::GFP intensity for
414 these differences to fully explain the highly non-overlapping differences between the quiescence

415 phenotype of the different strains. Surprisingly, *affl-1(sy1202)* worms have more granules per
416 nucleus after heat shock compared to wild-type worms ($p = 0.0016$) and the most number of
417 granules compared to the other mutants. *affl-2(sy975)* mutants formed slightly less granules after
418 heat shock ($p = 0.034$), and *affl-2(sy975) affl-1(sy1220)* mutants formed similar numbers of
419 granules per nucleus as wild type ($p = 0.883$). These results do not explain why *affl-2(sy975)*
420 worms are unable to express *hsp-16.41*, for some wild type worms had similar HSF1 granule
421 numbers per nuclei and similar HSF-1::GFP levels. Since HSF-1 localization and expression is
422 not significantly disrupted in *affl-2* mutants, we believe that AFFL-2 acts either downstream or
423 parallel to HSF-1 to regulate heat shock induced transcription in *C. elegans*. This suggests a
424 predicted role of *affl-2* in elongation, based on its homology with AF4/FMR2 family members.

425 **Discussion**

426 We have cloned and performed a genetic analysis of *affl-2*, a homolog of AF4/FMR2
427 family members and showed that *affl-2* is necessary for heat shock induced transcription.
428 Through a forward genetic screen for suppressors of heat shock induced *lin-3* overexpression, we
429 identified one new *hsf-1* and three *affl-2* alleles. To our knowledge, this is the first isolated viable
430 *hsf-1* allele with an altered DNA binding domain. We found that *affl-2* mutants are Dpy, Egl, and
431 have herniated intestines, whereas animals lacking a functional *affl-1*—a homolog of AF4/FMR2
432 family members and the paralog of *affl-2*— appear wild type. We determined that *affl-2* is a
433 ubiquitously expressed nuclear protein, and proper localization is necessary for its role in heat
434 shock induced transcriptional response.

435 *affl-2* mutants had been identified in another screen for suppressors of heat shock induced
436 gene expression, and that screen also identified *hsf-1* and *cyl-1* as regulators of heat shock
437 response (Hajdu-Cronin *et al.* 2004). As said above, we found an *hsf-1* mutant, but we did not
438 recover any *cyl-1* mutants. However, Hajdu-Cronin *et al.* (2004) reported that their *cyl-1* mutants
439 did not suppress the effects of a *Phsp-16.41* driven transgene, which indicate that *cyl-1* is not
440 responsible for *hsp-16.41* transcription. Hadju-Cronin's efforts and ours illustrate the power of
441 simple genetic screens for gene expression in *C. elegans* to find genes responsible for regulation
442 of transcription.

443 Along with conservation in the CHD, we see a partial conservation of AFF4's AF9/ENL,
444 ELL-1/2, and P-TEFb binding sites in the AFFL-2 N terminal sequence (Fig 2C). AFFL-2 is
445 predicted computationally to have three candidates for binding sites, but we have not yet verified
446 whether these are real. It is possible that these three sites are sufficient for AFFL-2 to bind to its
447 partners in the SEC, and it is possible that AFFL-2 does not interact with all components of the

448 SEC that human AFF4/AFF1 have been found to bind. Our deletion removed the region of
449 AFFL-2 similar to AFF4's binding site to P-TEFb, and thus we expected it to be necessary for
450 the AFFL-2's function. Surprisingly, we found that replacing much of the disordered N-terminus
451 of AFFL-2 with an exogenous NLS restores protein function to about 80% of the wild-type
452 control, even though the modified AFFL-2 with its predicted NLSs at the N-terminus removed
453 still partially localizes to the nucleus. It is possible that the C-terminus of AFFL-2 may contain a
454 weak NLS that cannot be predicted by current software which allows AFFL-2 to partially
455 localize to the nucleus at low levels. Addition of an exogenous NLS could be necessary to
456 increase the concentration of nuclear AFFL-2 to improve its functioning, but does not restore
457 AFFL-2 activity to wild-type levels. Our deleted residues removed only one of the candidate
458 binding sites of AFFL-2, and it is possible that the other binding sites and disordered residues
459 can act redundantly to maintain AFFL-2 activity. However, a more thorough biochemical
460 investigation of AFFL-2 is needed to determine the role of different domains of the protein.

461 Despite AFFL-1 being an ortholog of AFF4/AFF1 as well, AFFL-1 is not necessary for
462 heat shock induced transcription and *affl-1* mutants appear wild type. AFFL-1 is not predicted to
463 have any Nuclear Localization Signals, which suggests that it may not even be a nuclear protein.
464 Since we do not have a phenotype for *affl-1* mutants we have no way to validate any expression
465 pattern or localization obtained using a fusion protein, for we cannot validate that the fusion
466 protein is functional. It is not clear what AFFL-1's role is, and if AFFL-1 has a role in
467 transcription or not. We have not fully investigated *affl-1* mutants to see if they have any
468 deficiencies in other processes besides heat shock induced transcription, and *affl-1* could play a
469 redundant role with another gene.

470 We used translational reporters to examine the roles of *affl-1* and *affl-2* on HSF-1
471 subcellular localization and expression. While we did find some differences in HSF-1 expression
472 prior to heat shock and HSF-1 granule formation after heat shock, we are not confident that these
473 differences can explain the phenotypes of the various mutants because the distributions of our
474 measurements for different genotypes overlap. This aligns with our hypothesis that *affl-2* is
475 necessary for proper elongation in transcription, not initiation, for it suggests that AFFL-2 acts
476 downstream of granule formation. Furthermore, addition of the FUS LC domain does not
477 significantly increase the performance of the modified AFFL-2, which suggests that AFFL-2 is
478 not involved in recruiting RNA polymerase but is acts in a downstream step. However, there are
479 no putative binding sites for the granules and it is unclear what their role in heat shock response
480 is (Morton and Lamitina 2013).

481 As mentioned previously, AFFL-1 and AFFL-2 are homologs of mammalian AFF1 and
482 AFF4, which serve as scaffolds for the super elongation complex (SEC). AFF1 and AFF4 serve
483 as scaffolds in the super elongation complex (SEC), which regulates release from promoter-
484 proximal pausing during transcriptional elongation using P-TEFb (He and Zhou 2011; Lu *et al.*
485 2014; Mück *et al.* 2016). AFF4 is responsible for heat shock induced HSP70 expression, which
486 illustrates that its role in heat shock induced gene expression is conserved (Lu *et al.* 2015). In *C.*
487 *elegans*, the P-TEFb complex has been shown to be necessary for embryonic development and
488 expression of *hsp-16.2* (Schulze-Gahmen *et al.* 2013). Although *affl-2* and *affl-1* mutants survive
489 past embryonic development, *affl-2* mutants are deficient in heat shock induced gene expression.
490 Future work should investigate whether *affl-2* mutants are also deficient in expression of genes
491 involved in embryonic development and whether they have the same defects in Ser2
492 phosphorylation as animals lacking a function P-TEFb complex (Schulze-Gahmen *et al.* 2013).It

493 is possible that *affl-2* mutants still have Ser2 phosphorylation, but at lower levels than wild type,
494 which could allow them able to survive through development.

495 Our results demonstrate that the *C. elegans* ortholog of AF4/FMR2 family members,
496 AFFL-2, is necessary for heat shock induced transcription. Our sequence analysis suggests that
497 AF4/FMR2 homologues are found more widely in nature than previously thought, highlighting
498 their importance. These results combined with previous work on other members of the SEC
499 suggest that *C. elegans* can be a powerful, multicellular model to understand transcriptional
500 elongation. Further study of *C. elegans* homologs of human AF4/FMR2 proteins will facilitate
501 our understanding of heat shock response as well as transcriptional elongation in general.

502

503

504 **Acknowledgements**

505 We thank Heenam Park for helping create *Y55B1BR.1 (affl-1)* null mutants using CRISPR/Cas9,
506 and we thank Jean Badroos, Jasmine S. Revanna, and Minyi Tan for technical assistance. We
507 thank Hillel Schwartz, Jonathan Liu, and members of the Sternberg Lab for insightful
508 discussions. We thank Sarah MacLean and the Sternberg Lab for comments on the manuscript.
509 Some strains were provided by the CGC, which is funded by NIH Office of Research
510 Infrastructure Programs (P40 OD010440). This work was supported by NIH (K99GM126137 to
511 H.W., U24HG002223 to P.W.S., and R240D023041). The Millard and Muriel Jacobs Genetics
512 and Genomics Laboratory at California Institute of Technology performed whole genome
513 sequencing. S.J.W. was supported by the Caltech Student Faculty Programs, the family of
514 Laurence J. Stuppy, Samuel N. Vodopia, and Carol J. Hasson.

515

516 **Data Availability.**

517 Strains and plasmids are available upon request. Code for data analysis and image processing can
518 be found at: <https://github.com/sophiejwalton/affl-2.git>. Data will be made publicly available
519 upon publication.

520

521

522

523 **References**

- 524 Åkerfelt M., R. I. Morimoto, and L. Sistonen, 2010 Heat shock factors: integrators of cell stress,
525 development and lifespan. *Nature Reviews Molecular Cell Biology* 11: 545–555.
526 <https://doi.org/10.1038/nrm2938>
- 527 Arvand A., and C. T. Denny, 2001 Biology of EWS/ETS fusions in Ewing’s family tumors.
528 *Oncogene* 20: 5747–5754. <https://doi.org/10.1038/sj.onc.1204598>
- 529 Bois J., 2018 *bebi103*.
- 530 Bowman E. A., C. R. Bowman, J. H. Ahn, and W. G. Kelly, 2013 Phosphorylation of RNA
531 polymerase II is independent of P-TEFb in the *C. elegans* germline. *Development* 140:
532 3703–3713. <https://doi.org/10.1242/dev.095778>
- 533 Brenner S., 1974 The Genetics of *Caenorhabditis Elegans*. *Genetics* 77: 71–94.
- 534 Cai L., B. L. Phong, A. L. Fisher, and Z. Wang, 2011 Regulation of Fertility, Survival, and
535 Cuticle Collagen Function by the *Caenorhabditis elegans* eaf-1 and ell-1 Genes. *J. Biol.*
536 *Chem.* 286: 35915–35921. <https://doi.org/10.1074/jbc.M111.270454>
- 537 Chen Y., and P. Cramer, 2019 Structure of the super-elongation complex subunit AFF4 C-
538 terminal homology domain reveals requirements for AFF homo- and heterodimerization.
539 *J. Biol. Chem.* 294: 10663–10673. <https://doi.org/10.1074/jbc.RA119.008577>
- 540 Chou S., H. Upton, K. Bao, U. Schulze-Gahmen, A. J. Samelson, *et al.*, 2013 HIV-1 Tat recruits
541 transcription elongation factors dispersed along a flexible AFF4 scaffold. *PNAS* 110:
542 E123–E131. <https://doi.org/10.1073/pnas.1216971110>

- 543 Doitsidou M., R. J. Poole, S. Sarin, H. Bigelow, and O. Hobert, 2010 *C. elegans* Mutant
544 Identification with a One-Step Whole-Genome-Sequencing and SNP Mapping Strategy.
545 PLoS One 5. <https://doi.org/10.1371/journal.pone.0015435>
- 546 Dosztányi Z., V. Csizmok, P. Tompa, and I. Simon, 2005 IUPred: web server for the prediction
547 of intrinsically unstructured regions of proteins based on estimated energy content.
548 Bioinformatics 21: 3433–3434. <https://doi.org/10.1093/bioinformatics/bti541>
- 549 Dosztányi Z., B. Mészáros, and I. Simon, 2009 ANCHOR: web server for predicting protein
550 binding regions in disordered proteins. Bioinformatics 25: 2745–2746.
551 <https://doi.org/10.1093/bioinformatics/btp518>
- 552 Dosztanyi Z., B. Meszaros, and G. Erdos, 2018 *IUPred2a*. MTA-ELTE Momentum
553 Bioinformatics Research Group.
- 554 Edgar R. C., 2004 MUSCLE: multiple sequence alignment with high accuracy and high
555 throughput. Nucleic Acids Res 32: 1792–1797. <https://doi.org/10.1093/nar/gkh340>
- 556 Gopalan S., D. M. Gibbon, C. A. Banks, Y. Zhang, L. A. Florens, *et al.*, 2018
557 *Schizosaccharomyces pombe* Pol II transcription elongation factor ELL functions as part
558 of a rudimentary super elongation complex. Nucleic Acids Res 46: 10095–10105.
559 <https://doi.org/10.1093/nar/gky713>
- 560 Guipaud O., F. Guillonneau, V. Labas, D. Praseuth, J. Rossier, *et al.*, 2006 An in vitro enzymatic
561 assay coupled to proteomics analysis reveals a new DNA processing activity for Ewing
562 sarcoma and TAF(II)68 proteins. PROTEOMICS 6: 5962–5972.
563 <https://doi.org/10.1002/pmic.200600259>

- 564 Hajdu-Cronin Y. M., W. J. Chen, and P. W. Sternberg, 2004 The L-type cyclin CYL-1 and the
565 heat-shock-factor HSF-1 are required for heat-shock-induced protein expression in
566 *Caenorhabditis elegans*. *Genetics* 168: 1937–1949.
567 <https://doi.org/10.1534/genetics.104.028423>
- 568 He N., and Q. Zhou, 2011 New Insights into the Control of HIV-1 Transcription: When Tat
569 Meets the 7SK snRNP and Super Elongation Complex (SEC). *J Neuroimmune*
570 *Pharmacol* 6: 260–268. <https://doi.org/10.1007/s11481-011-9267-6>
- 571 Jones D., R. H. Russnak, R. J. Kay, and E. P. Candido, 1986 Structure, expression, and evolution
572 of a heat shock gene locus in *Caenorhabditis elegans* that is flanked by repetitive
573 elements. *J. Biol. Chem.* 261: 12006–12015.
- 574 Jones E., T. Oliphant, P. Peterson, and et. al, 2001 *SciPy: Open Source Scientific Tools for*
575 *Python*.
- 576 Kosugi S., M. Hasebe, T. Entani, S. Takayama, M. Tomita, *et al.*, 2008 Design of peptide
577 inhibitors for the importin alpha/beta nuclear import pathway by activity-based profiling.
578 *Chem. Biol.* 15: 940–949. <https://doi.org/10.1016/j.chembiol.2008.07.019>
- 579 Kosugi S., M. Hasebe, N. Matsumura, H. Takashima, E. Miyamoto-Sato, *et al.*, 2009a Six
580 classes of nuclear localization signals specific to different binding grooves of importin
581 alpha. *J. Biol. Chem.* 284: 478–485. <https://doi.org/10.1074/jbc.M807017200>
- 582 Kosugi S., M. Hasebe, M. Tomita, and H. Yanagawa, 2009b Systematic identification of cell
583 cycle-dependent yeast nucleocytoplasmic shuttling proteins by prediction of composite

- 584 motifs. Proc. Natl. Acad. Sci. U.S.A. 106: 10171–10176.
585 <https://doi.org/10.1073/pnas.0900604106>
- 586 Kuras L., and K. Struhl, 1999 Binding of TBP to promoters in vivo is stimulated by activators
587 and requires Pol II holoenzyme. Nature 399: 609–613. <https://doi.org/10.1038/21239>
- 588 Kwon I., M. Kato, S. Xiang, L. Wu, P. Theodoropoulos, *et al.*, 2013 Phosphorylation-Regulated
589 Binding of RNA Polymerase II to Fibrous Polymers of Low-Complexity Domains. Cell
590 155: 1049–1060. <https://doi.org/10.1016/j.cell.2013.10.033>
- 591 Leach B. I., A. Kuntimaddi, C. R. Schmidt, T. Cierpicki, S. A. Johnson, *et al.*, 2013 Leukemia
592 Fusion Target AF9 Is an Intrinsically Disordered Transcriptional Regulator that Recruits
593 Multiple Partners via Coupled Folding and Binding. Structure 21: 176–183.
594 <https://doi.org/10.1016/j.str.2012.11.011>
- 595 Lenasi T., and M. Barboric, 2010 P-TEFb stimulates transcription elongation and pre-mRNA
596 splicing through multilateral mechanisms. RNA Biology 7: 145–150.
597 <https://doi.org/10.4161/rna.7.2.11057>
- 598 Lessnick S. L., and M. Ladanyi, 2012 Molecular Pathogenesis of Ewing Sarcoma: New
599 Therapeutic and Transcriptional Targets. Annu. Rev. Pathol. Mech. Dis. 7: 145–159.
600 <https://doi.org/10.1146/annurev-pathol-011110-130237>
- 601 Levine M., 2011 Paused RNA Polymerase II as a Developmental Checkpoint. Cell 145: 502–
602 511. <https://doi.org/10.1016/j.cell.2011.04.021>

- 603 Li J., L. Chauve, G. Phelps, R. M. Briemann, and R. I. Morimoto, 2016 E2F coregulates an
604 essential HSF developmental program that is distinct from the heat-shock response.
605 *Genes Dev.* 30: 2062–2075. <https://doi.org/10.1101/gad.283317.116>
- 606 Lin C., E. R. Smith, H. Takahashi, K. C. Lai, S. Martin-Brown, *et al.*, 2010 AFF4, a Component
607 of the ELL/P-TEFb Elongation Complex and a Shared Subunit of MLL Chimeras, Can
608 Link Transcription Elongation to Leukemia. *Molecular Cell* 37: 429–437.
609 <https://doi.org/10.1016/j.molcel.2010.01.026>
- 610 Lin C., A. S. Garrett, B. D. Kumar, E. R. Smith, M. Gogol, *et al.*, 2011 Dynamic transcriptional
611 events in embryonic stem cells mediated by the super elongation complex (SEC). *Genes*
612 *Dev.* 25: 1486–1498. <https://doi.org/10.1101/gad.2059211>
- 613 Lu H., Z. Li, Y. Xue, U. Schulze-Gahmen, J. R. Johnson, *et al.*, 2014 AFF1 is a ubiquitous P-
614 TEFb partner to enable Tat extraction of P-TEFb from 7SK snRNP and formation of
615 SECs for HIV transactivation. *PNAS* 111: E15–E24.
616 <https://doi.org/10.1073/pnas.1318503111>
- 617 Lu H., Z. Li, W. Zhang, U. Schulze-Gahmen, Y. Xue, *et al.*, 2015 Gene target specificity of the
618 Super Elongation Complex (SEC) family: how HIV-1 Tat employs selected SEC
619 members to activate viral transcription. *Nucleic Acids Res* 43: 5868–5879.
620 <https://doi.org/10.1093/nar/gkv541>
- 621 Luo Z., C. Lin, E. Guest, A. S. Garrett, N. Mohagheh, *et al.*, 2012a The Super Elongation
622 Complex Family of RNA Polymerase II Elongation Factors: Gene Target Specificity and

- 623 Transcriptional Output. *Molecular and Cellular Biology* 32: 2608–2617.
- 624 <https://doi.org/10.1128/MCB.00182-12>
- 625 Luo Z., C. Lin, and A. Shilatifard, 2012b The super elongation complex (SEC) family in
626 transcriptional control. *Nature Reviews Molecular Cell Biology* 13: 543–547.
- 627 <https://doi.org/10.1038/nrm3417>
- 628 Maier W., K. Moos, M. Seifert, and R. Baumeister, 2014 *MiModD - Mutation Identification in*
629 *Model Organism Genomes*. SourceForge.net.
- 630 Morimoto R. I., 1998 Regulation of the heat shock transcriptional response: cross talk between a
631 family of heat shock factors, molecular chaperones, and negative regulators. *Genes Dev.*
632 12: 3788–3796. <https://doi.org/10.1101/gad.12.24.3788>
- 633 Morton E. A., and T. Lamitina, 2013 *C. elegans* HSF-1 is an essential nuclear protein that forms
634 stress granule-like structures following heat shock. *Aging Cell* 12: 112–120.
- 635 <https://doi.org/10.1111/accel.12024>
- 636 Mück F., S. Bracharz, and R. Marschalek, 2016 DDX6 transfers P-TEFb kinase to the
637 AF4/AF4N (AFF1) super elongation complex. *Am J Blood Res* 6: 28–45.
- 638 Oliver Hobert Lab, Worm Genomic DNA Prep
- 639 Potter S. C., A. Luciani, S. R. Eddy, Y. Park, R. Lopez, *et al.*, 2018 HMMER web server: 2018
640 update. *Nucleic Acids Res* 46: W200–W204. <https://doi.org/10.1093/nar/gky448>

- 641 Qi S., Z. Li, U. Schulze-Gahmen, G. Stjepanovic, Q. Zhou, *et al.*, 2017 Structural basis for ELL2
642 and AFF4 activation of HIV-1 proviral transcription. *Nature Communications* 8: 14076.
643 <https://doi.org/10.1038/ncomms14076>
- 644 Richter K., M. Haslbeck, and J. Buchner, 2010 The Heat Shock Response: Life on the Verge of
645 Death. *Molecular Cell* 40: 253–266. <https://doi.org/10.1016/j.molcel.2010.10.006>
- 646 Saunders A., L. J. Core, and J. T. Lis, 2006 Breaking barriers to transcription elongation. *Nat*
647 *Rev Mol Cell Biol* 7: 557–567. <https://doi.org/10.1038/nrm1981>
- 648 Schindelin J., I. Arganda-Carreras, E. Frise, V. Kaynig, M. Longair, *et al.*, 2012 Fiji: an open-
649 source platform for biological-image analysis. *Nat Methods* 9: 676–682.
650 <https://doi.org/10.1038/nmeth.2019>
- 651 Schulze-Gahmen U., H. Upton, A. Birnberg, K. Bao, S. Chou, *et al.*, 2013 The AFF4 scaffold
652 binds human P-TEFb adjacent to HIV Tat. *eLife*.
- 653 Schulze-Gahmen U., H. Lu, Q. Zhou, and T. Alber, 2014 AFF4 binding to Tat-P-TEFb indirectly
654 stimulates TAR recognition of super elongation complexes at the HIV promoter. *eLife*.
- 655 Schulze-Gahmen U., and J. H. Hurley, 2018 Structural mechanism for HIV-1 TAR loop
656 recognition by Tat and the super elongation complex. *PNAS* 115: 12973–12978.
657 <https://doi.org/10.1073/pnas.1806438115>
- 658 Shim E. Y., A. K. Walker, Y. Shi, and T. K. Blackwell, 2002 CDK-9/cyclin T (P-TEFb) is
659 required in two postinitiation pathways for transcription in the *C. elegans* embryo. *Genes*
660 *Dev.* 16: 2135–2146. <https://doi.org/10.1101/gad.999002>

- 661 Sims R. J., R. Belotserkovskaya, and D. Reinberg, 2004 Elongation by RNA polymerase II: the
662 short and long of it. *Genes Dev.* 18: 2437–2468. <https://doi.org/10.1101/gad.1235904>
- 663 Van Buskirk C., and P. W. Sternberg, 2007 Epidermal growth factor signaling induces
664 behavioral quiescence in *Caenorhabditis elegans*. *Nature Neuroscience* 10: 1300–1307.
665 <https://doi.org/10.1038/nm1981>
- 666 Voellmy R., and F. Boellmann, 2007 Chaperone Regulation of the Heat Shock Protein Response,
667 pp. 89–99 in *Molecular Aspects of the Stress Response: Chaperones, Membranes and*
668 *Networks*, *Advances in Experimental Medicine and Biology*. edited by Csermely P.,
669 Vígth L. Springer New York, New York, NY.
- 670 Walt S. van der, J. L. Schönberger, J. Nunez-Iglesias, F. Boulogne, J. D. Warner, *et al.*, 2014
671 scikit-image: image processing in Python. *PeerJ* 2: e453.
672 <https://doi.org/10.7717/peerj.453>
- 673 Wang H., J. Liu, S. Gharib, C. M. Chai, E. M. Schwarz, *et al.*, 2017 cGAL, a temperature-robust
674 GAL4–UAS system for *Caenorhabditis elegans*. *Nature Methods* 14: 145–148.
675 <https://doi.org/10.1038/nmeth.4109>
- 676 Wang H., H. Park, J. Liu, and P. W. Sternberg, 2018 An Efficient Genome Editing Strategy To
677 Generate Putative Null Mutants in *Caenorhabditis elegans* Using CRISPR/Cas9. *G3:*
678 *Genes, Genomes, Genetics* 8: 3607–3616. <https://doi.org/10.1534/g3.118.200662>
- 679 Zhou Q., T. Li, and D. H. Price, 2012 RNA Polymerase II Elongation Control. *Annu. Rev.*
680 *Biochem.* 81: 119–143. <https://doi.org/10.1146/annurev-biochem-052610-095910>

682 **Supporting Information**

683 **Supplementary Data:**

684 Figure S1: *sup-45* (Y55B1BR.2) SNP mapping data.

685 Figure S2: Alignment of example AF4/FMR2 C-terminal Homology Domains.

686 Figure S3: Subcellular Localization of AFFL-2 N-terminal Deletion::GFP.

687 Figure S4: Morphology of AFFL-2 rescue variants.

688 Figure S5: Quantification of HSF-1::GFP in various mutants.

689 **Supplementary Experimental Procedures:**

690 **Appendix 1: Strains Used in This Study**

691 Table S1: Mutant Strains

692 Table S2: Strains used for *affl-2* expression experiments

693 Table S3: Strains used for *affl-2* rescue variants

694 Table S4: Strains for HSF-1::GFP localization experiments

695 **Appendix 2: Plasmids created for this study**

696 Table S5: pSJW003 Construction

697 Table S6: pSJW005 Construction

698 Table S7: pSJW0035 Construction

699 Table S8: pSJW0036 Construction

700 Table S9: pSJW0040 Construction

701 Table S10: pSJW0041 Construction

702 **Appendix 3: Oligos for genotyping used in this study**

703 **Tables**

704 **Table 1: DNA Sequence Changes of Alleles**

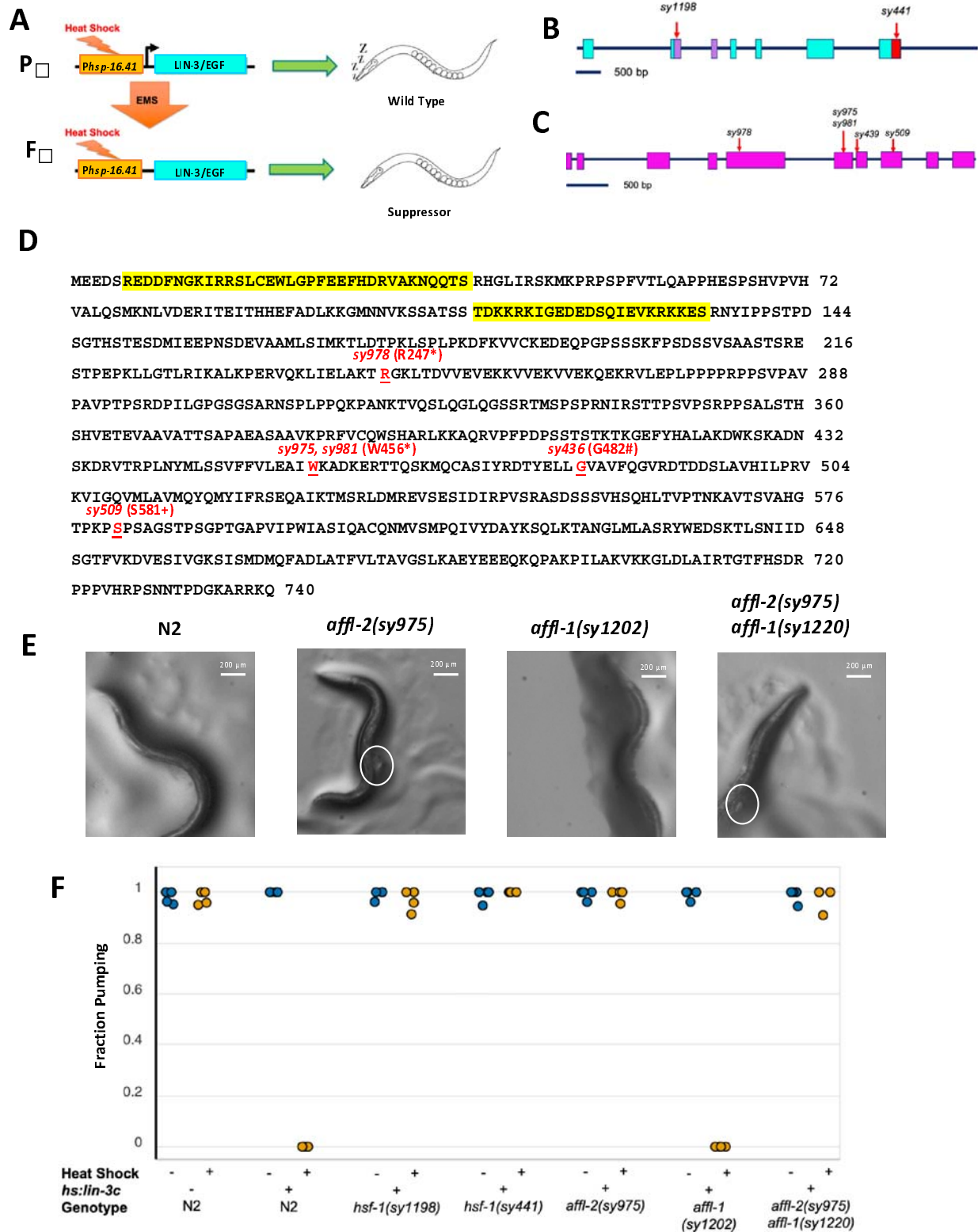
Allele	Sequence change with 25 base pair flanking sequence around the mutation (bold letter)	Predicted Amino Acid Change
<i>hsf-1(sy1198)</i>	GACGACGACAAGCTTCCAGTATTC AGATAAAATTGTGGAATATCGTAGAA	L93Q
<i>affl-2(sy978)</i>	GAAGCTCATTGAGCTTGCGAAGACC TGAGGGAAAGCTGACGGATGTTGTGGA	R247*
<i>affl-2(sy981)</i>	GTATTTTTTGTACTTGAAGCCATCT AGAAAGCTGACAAGGAGCGGACAAC T	W456*
<i>affl-2(sy975)</i>	TATTTTTTGTACTTGAAGCCATCTG AAAAGCTGACAAGGAGCGGACAAC TC	W456*
<i>affl-2(sy509)</i>	AGTGGCTCACGGGACCCCAAACCA ACCCACGTCCGCGGATCGACACC ATCTGGT	Missense mutations starting at S581 R635* and from to frameshift caused by CC to CAC mutation.
<i>affl-2(sy439)</i>	tttataaaattgatgaataattca AGTCGCCGTGTTTCAAGGTGTCCGC	Altered splice acceptor site before G482

705

706 **Table 1: DNA Sequence Changes of Alleles.** Alleles *sy439* and *sy509* were both identified in
707 Hadju-Cronin et. al (2004), where *affl-2* was named *sup-45*. All other alleles were identified in
708 this screen. Bold letters indicate modified bp(s) in that allele. Uppercase represents exons and
709 lowercase represents introns.

710

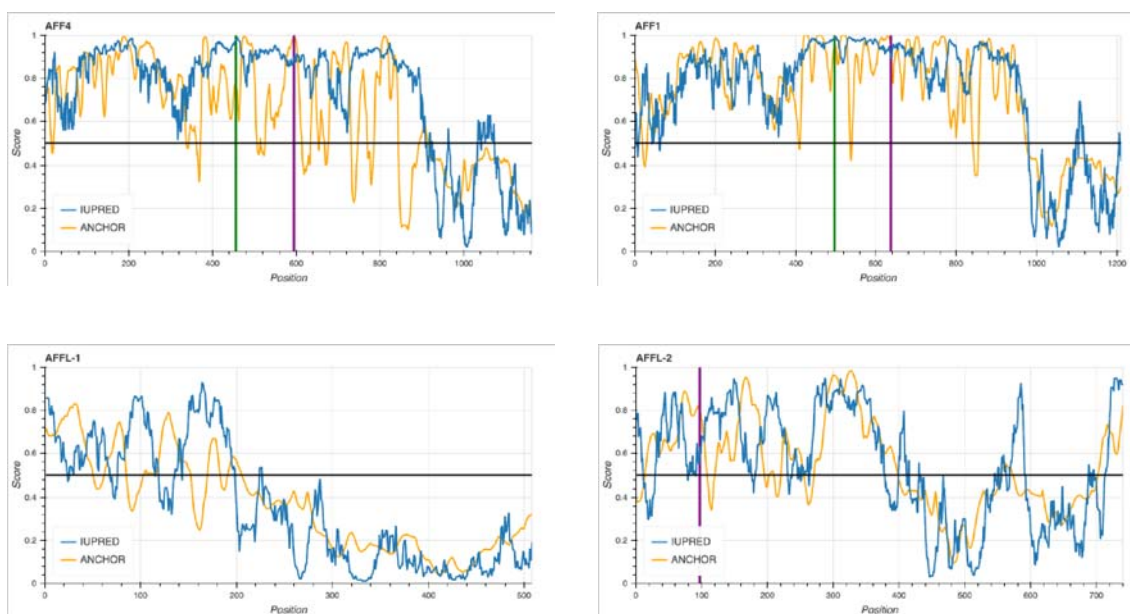
711 **Figures:**



713 **Figure 1. *hsf-1* and *affl-2* were discovered in a screen for suppressors of heat shock induced**
714 ***lin-3c* overexpression.** (A) Outline of screening process. The F2 progeny of mutagenized Phsp-
715 16.41:*lin3-c* animals were screened for suppression of *lin-3c* overexpression induced pumping
716 quiescence. Gene diagrams of *hsf-1* (B) and *affl-2* (C). Blocks are exons, lines are introns, and
717 red arrows indicate position of molecular changes for alleles. Sequences for alleles can be found
718 in table 1. (D) Annotated AFFL-2 sequence. Highlighted text in yellow corresponds to predicted
719 NLSs, and disrupted residue due to allele change is underlined in red text. * indicates stop; #
720 indicates splice site disruption prior to residue; + indicates first disrupted residue of missense
721 mutation and frameshift caused by *sy509*. (E) Images of wild type (N2), *affl-2* mutant, *affl-1*
722 mutant, and *affl-2 affl-1* double mutants. Protruding intestines from vulvas are circled. (F)
723 Fraction of worms pumping before or after heat shock to induce *hsp-16.41: lin-3c* expression.
724 Data are a proxy for gene expression (pumping quiescence indicates *hsp-16.41* expression). Each
725 point represents a different trial.
726
727

728

A



729

B

```

Affi-2_CAEL1/1-740      1 MEE-----DSLEDDFNCKIRRS LCEWLGPFEEFHDRVAKNQQTSLHGLIRSKM-KP----- 51
Aff1_HUMAN/1-1210     1 MAAQSSLYNDDRNLLRIR EKERRNQEAHQEKAFPEKIPLGFEPYK-TACDELSSLIQ----NMLGNVEVKEFLSTKSHTHLDASENR LCKPKYPLI 95
Affi-1_CAEL1/1-508     1 MKS-----GKPLP----- 9
Aff4_HUMAN/1-1163      1 -----MNR EDNRVLRMKERERRNQEIQQGEDAF PPSPLFAEPYKVTSLKLSLIQ----SMLGNVDEMKIFIGDRS-IPQLVA-----TPKPTVPPS 85

Affi-2_CAEL1/1-740      52 -----PSFYTLLQAPPHEPSHPV-----HVALQSMKNLVDERITEITHHFAADKKGM-----AKSCGPRDSQHLTQDRLLQEGFSSHHKKGD 101
Aff1_HUMAN/1-1210     179 RRADGDHCAVVDAPAELELSLILSLSPVPLSLPISHSNQTLPTQGSVVMGSSNNKGYCAASPKDLAVKVHDKETQDLSVAAPQPSQTFPPPS 178
Affi-1_CAEL1/1-508     86 -----HTSRSLSPV-CGLRTRRMLLEMAGLVGTKRLSGLRRLRFEDLQD-----LSQLRRLRFEDLQD----- 51
Aff4_HUMAN/1-1163      10 ADEKSN-PNFFQRHGGSGSKWPKV-GE-----AS-----TSQSQKSSGLQSGHSSQRTSAGSSSGTNSGQRHDRSEYNNSSSRKKGQ 168

Affi-2_CAEL1/1-740      102 -----NNVKSATSSSDK-----KIGEDSDQIEVKRKK-----ERNYIPF 141
Aff1_HUMAN/1-1210     179 RRADGDHCAVVDAPAELELSLILSLSPVPLSLPISHSNQTLPTQGSVVMGSSNNKGYCAASPKDLAVKVHDKETQDLSVAAPQPSQTFPPPS 278
Affi-1_CAEL1/1-508     52 -----DSATSPSD-----WNWMEKESY-----ESLITPFF 82
Aff4_HUMAN/1-1163      169 H-----GSEHKLRSSPG-----QAVSSLNSSH-----SISGNDHHEKHEQRSRPRDDA-----NWDSPSRVFSQHSIQGFPP 241

Affi-2_CAEL1/1-740      142 TFDSTH-----STE DMI EFNDEVAAMLSIMTID--TPKLSPLK 183
Aff1_HUMAN/1-1210     279 LPKSVAMQKQTAYVRFMDGQQAPESESELKPLLEDYRQQT--EKTDLKVPKAKLTKLMPQSQVQTYNEVHCVETLEMTHSWPPPLTAINT 376
Affi-1_CAEL1/1-508     83 SVSNTS-----K SATGLTPK--AGNLHSDQNLSCS-KPKITPVVK 326
Aff4_HUMAN/1-1163      242 LMSKSN SMLQKQTAYVRFMDGQ-----ESMEPLKSSSEHYSSQSHGNSMT ELKRLSSKAHLTKLIPQLDASA GDVSCVDEITLMTHSWPPPLTAINT 334

Affi-2_CAEL1/1-740      184 DFKVYCKEDEQGPSSKFPSSDSVSAASTSRE-----STP--EPKLLGTIRIKALKPE 235
Aff1_HUMAN/1-1210     468 -----EPKFPPEKDGQHMSSVYVQNKQYDTSKTHSNSSQGTSSMLEDDQLSDS EDSSEQTPEKPPSSAPPSAARSDQSKDKPKVKIKGRRAAAS 467
Affi-1_CAEL1/1-508     125 -----APSAFLKPPSKRKSVE-----INP-----GTPRYI 152
Aff4_HUMAN/1-1163      337 CKT-----EPKFPPEKDGQHMSSVYVQNKQYDTSKTHSNSSQGTSSMLEDDQLSDS EDSSEQTPEKPPSSAPPSAARSDQSKDKPKVKIKGRRAAAS 419

Affi-2_CAEL1/1-740      236 RVQLLIELAKTRGKLT DYVEVEKVVVEKVEKRVLEPLPPP RPFSV-----LPPPPRPFPV----- 285
Aff1_HUMAN/1-1210     561 DPFKSSSKAPRAPPEAHPGK--RSCQKSAQQLPQRQT VGTQKPKPPVKSAAAGSRTSLQGEREPGLLYGSRDQSKDKPKVKIKGRRAAAS 560
Affi-1_CAEL1/1-508     163 -----PLSP-----PEPDIHARV-----LPQR----- 162
Aff4_HUMAN/1-1163      420 GADNSRDDSSHSSESSSSSESSSSSANEPSLSASREPEPPTNKWQLDNWLKVNHKVSSASSVDSNIPSSQYKKEER EQGTGNSYDTS 519

Affi-2_CAEL1/1-740      286 --PAVAVVTPSRDP-----ILGPGSGSANN-----SLPPQKPA NKVQS LQLQ 330
Aff1_HUMAN/1-1210     377 STA-----EPKFPPEKDGQHMSSVYVQNKQYDTSKTHSNSSQGTSSMLEDDQLSDS EDSSEQTPEKPPSSAPPSAARSDQSKDKPKVKIKGRRAAAS 656
Affi-1_CAEL1/1-508     163 -----PLSP-----PEPDIHARV-----LPQR----- 162
Aff4_HUMAN/1-1163      520 GPKETSATPRGRDKTIQKGSERGRQKSPAQSDSTTQRRTVQKQKPAKAAAE-PRGGLKIESE--TPVDLASSMPSKAAKGRKRNK 383

Affi-2_CAEL1/1-740      331 S SRTMSPFRNISTTPVSPRPSALS HSHVTEVAAVATTSAPAEASA AVKPRFVCQWSHAR----- 395
Aff1_HUMAN/1-1210     657 NEFPKPAVPPSSKPKKHSLLAPSKALSQPEAKNVEDRTPEHFALVPLTESQGP HSGSRTSGCRQAVVQEDS-RKDR LPLLRDTKLLSLRDT 755
Affi-1_CAEL1/1-508     184 --KPTPKDKELIT--VYGEQVLE-----RTFICKWNHAR----- 217
Aff4_HUMAN/1-1163      615 KESSSRRTAKKRYKSSKSSQKSR EILE--TSSSDSDESESLPP--SSQT KKPES-NRTB-VKPSVVEEDSFQRMFMSMEEKELLSLSE 708

Affi-2_CAEL1/1-740      396 -----LKKQIVP-----LQDLSRIPQPGKSRQRKAEDKQPPAKKHSSEKRSSDS-SSKLAKRKGAE-RDCDNKIRLEKEIKSQSSSSSSSHKESSKTKPS 403
Aff1_HUMAN/1-1210     756 PPKQLMVKITDLSRIPQPGKSRQRKAEDKQPPAKKHSSEKRSSDS-SSKLAKRKGAE-RDCDNKIRLEKEIKSQSSSSSSSHKESSKTKPS 853
Affi-1_CAEL1/1-508     218 -----LRVAQEV----- 225
Aff4_HUMAN/1-1163      709 DDRYLIVKIDNLNLTLPKRYKETEPKGEKKNVPEKHTREAQKASEKVS NKGRKHKHEDDNRASESKKKTED--KNSAGHKPSNRESK---- 802

Affi-2_CAEL1/1-740      404 -----FPDF-----SSTKTG----- 416
Aff1_HUMAN/1-1210     854 R SSSSKKEMLPF--PVSSSSQKPAKALKR SRREADTCCQDPK SASSTKSNHKDSSI PKQRVEKGR R SSSSHGSSGDTANFVSLN-GNS 950
Affi-1_CAEL1/1-508     226 -----VDF----- 235
Aff4_HUMAN/1-1163      803 --QSAEKD LPSAGVPSKDPKTEHGRKRTISQSSSLKSSNSNKETS SSKNSSSTSQKKT EKTSSKLVKAPASSSNCBPSA TLDSS 899

Affi-2_CAEL1/1-740      417 -----EFYHALADWVSKADN-SKDRVTPPLNMLSSVFFVLEAIWKADKERIQSKMQCAS YRDTYELLVAVFQGVDT--DLSLA 497
Aff1_HUMAN/1-1210     951 KPGKQYKFDKQ--QADLMRFAKMKQKAEI-MDRGQAFKML EAVLSIECGIATESSSSKRAE--SVSSSTVDLFEIM--SLG SF--SBATA 1040
Affi-1_CAEL1/1-508     236 -----EFYHALAEWRCQATLENMPLVIFL FMSVFFVLEAIWKADKERIQSKMQCAS YRDTYELLVAVFQGVDT--DLSLA 1040
Aff4_HUMAN/1-1163      900 KRRTKLVFDDRNSADHYLQEAALKLNADA-LSDFEAVYLDVAVSIECGNALEKNAE KSPF--PMYSETVDLIVYIM--KLNVLAPDATA 993

Affi-2_CAEL1/1-740      498 VHLLELVYKVGQVMLAVMQMIFPSQATITMSRLDMELVSESIDIRVSRASDSSVHSQHLVFTNKAVTSVAGTFFKPFPSAGSTPSGPTGAV 596
Aff1_HUMAN/1-1210     1041 PTEKTFVLCMRCEQILNMMFRCKKIAIHY-----SSTLNKHF-----SSKVAQAPSCIAL--TGTSPSPSPMPSASVSSQSSA 1120
Affi-1_CAEL1/1-508     319 AHFRLV KLLSLVML SVMQRMLLSNIFQMQTRLESVAGFIE-----NDLIE-----AHGALP LVSVSD-- 384
Aff4_HUMAN/1-1163      994 --ADKLT VILCRCE LLYRLFKLKNALRY--SKLTLEHK-----NLYNNQARS PGLSKAVGMPSPVSPKLSGNGYSSCA 1073

Affi-2_CAEL1/1-740      597 IWIATQACQNVVM--PILVMDAYKQLKTANGMLMADRVEDKTLNINIS ETVKVESIVGKSTSMNQ-FADLATFVLTAVGSLKAEYEEEQ 693
Aff1_HUMAN/1-1210     1121 --GSGSSVYAAEISTPTIONISYVTITSHVLEAFDLWEQREALR--KNEFFARLSNMC-TLALNBS-LVDLVHTRQGFQQLQ----- 1206
Affi-1_CAEL1/1-508     385 VEWSEWQKCKFVAM--PILVMDAYKQLKTANGMLMADRVEDKTLNINIS ETVKVESIVGKSTSMNQ-FADLATFVLTAVGSLKAEYEEEQ 481
Aff4_HUMAN/1-1163      1074 ----SASASGSVLI--PKIIMQAAVYQVTSNFWATLWDQAEQLK--RQEFFAE LDMVG-PLIFNASIMTDLVAKTRQLHLWLRD----- 1158

Affi-2_CAEL1/1-740      694 QAKI LAKVKKGLDLAIRTGFHSDRPPVHRPSNNTPDGKARRKQ 740
Aff1_HUMAN/1-1210     1207 -----RTE----- 1210
Affi-1_CAEL1/1-508     482 LVKRVLEEVQMRFNLAQFGA-----ALESN 508

```


731 **Figure 2. *affl-2* is a homolog of the AF4/FMR2 family and predicted to be a disordered**
732 **protein.** (A) Plots of ANCHOR and IUPRED score per residue for AFF4, AFF1, AFFL-1, and
733 AFFL-2. IUPRED predicts disordered residues, and higher scores indicate higher confidence that
734 a residue is disordered (Dosztányi *et al.* 2005; Dosztanyi *et al.* 2018). ANCHOR predicts
735 disordered protein binding regions, and higher scores indicate higher confidence that a
736 disordered residue can participate in protein binding (Dosztányi *et al.* 2009). (B) Diagram of *H.*
737 *sapiens* AFF4 with annotated binding sites (Chou *et al.* 2013; Leach *et al.* 2013; Schulze-
738 Gahmen *et al.* 2013, 2014; Qi *et al.* 2017; Schulze-Gahmen and Hurley 2018; Chen and Cramer
739 2019). (C) Sequence alignment of AFFL-2, AFF1-1 (AFFL-2's paralog in *C. elegans*), and AFF1
740 and AFF4 in *H. sapiens*. The alignment was prepared using Jalview with ClustalX coloring to
741 highlight conservation (Edgar 2004) , where conserved residues are colored as follows:
742 hydrophobic (blue), positive charge (red), negative charge (magenta), polar (green), cysteines
743 (pink), glycine (orange), proline (yellow) and aromatic (cyan). The UniProtKB accession
744 identifiers for each sequence are listed here: Affl-2_CAEEL, Q95XW7; Affl-1_CAEEL,
745 Q95XW6; AFF1_HUMAN, P51825; AFF4_HUMAN, Q9UHB7.

746

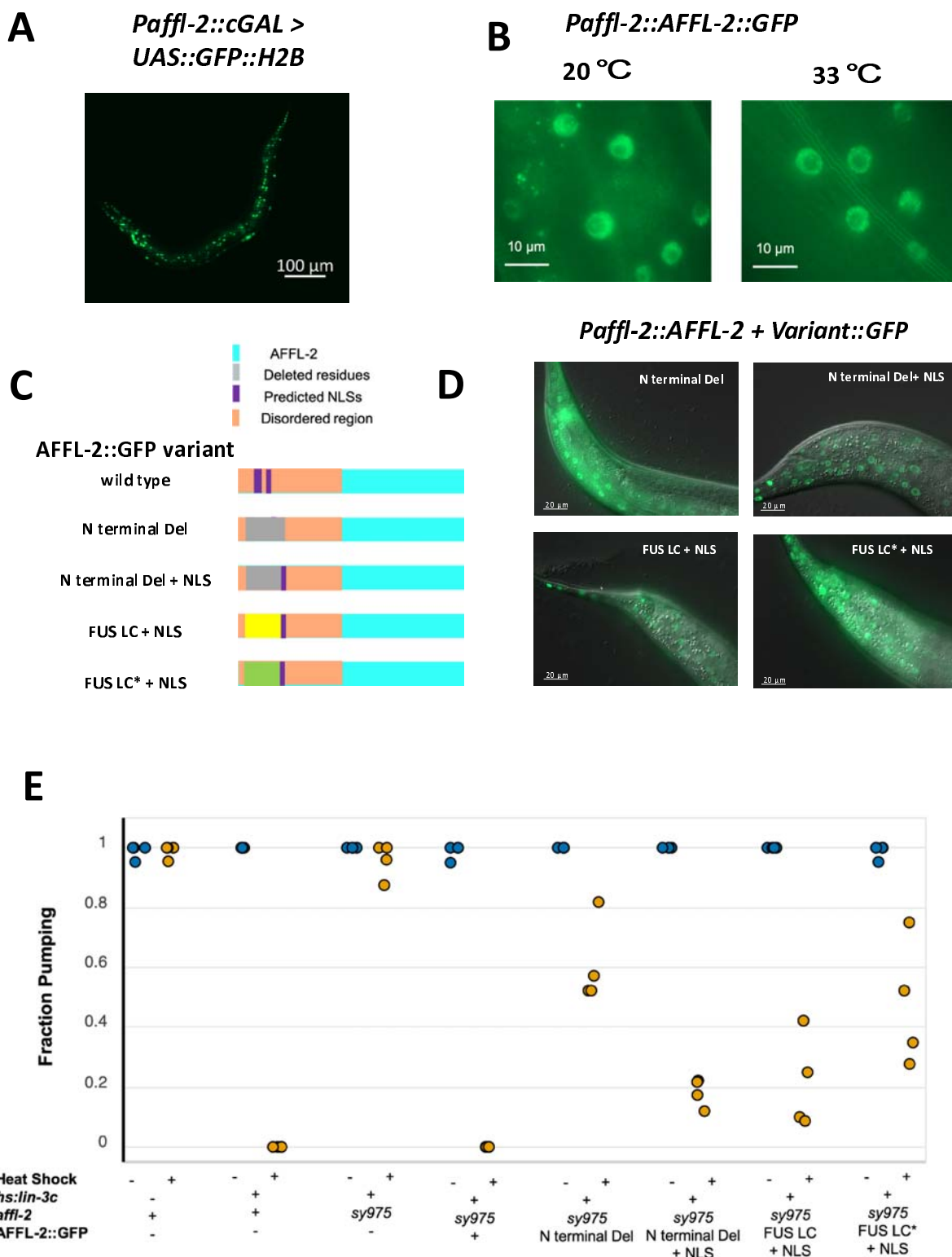
747

748

749

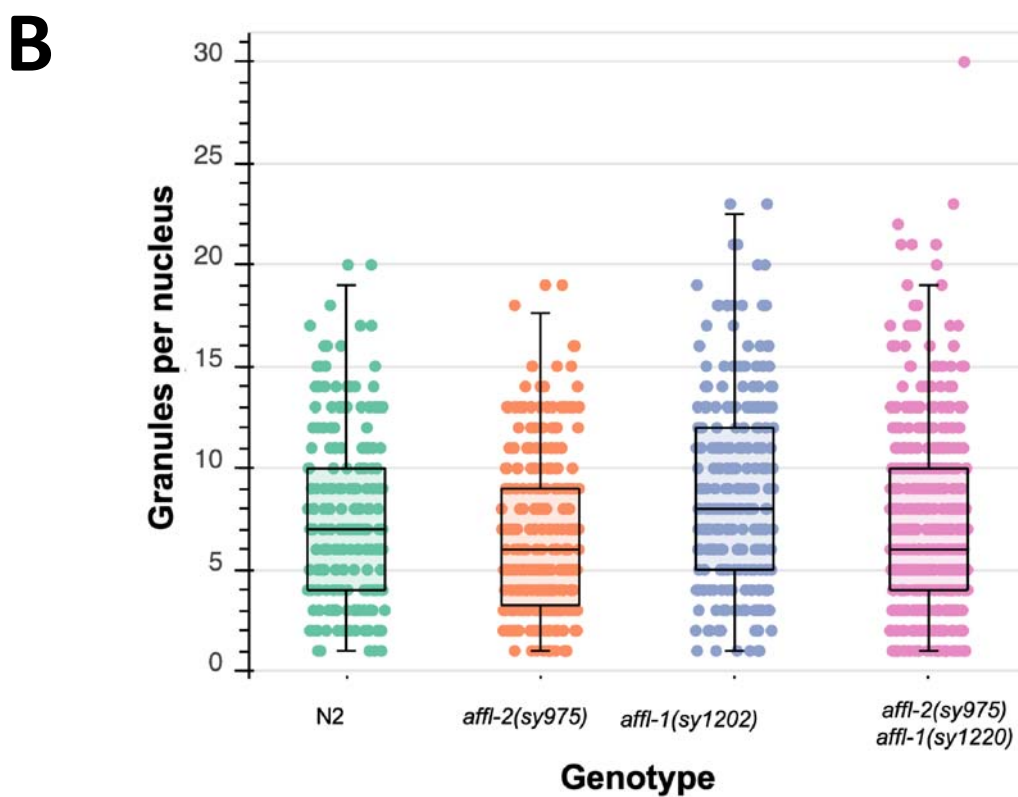
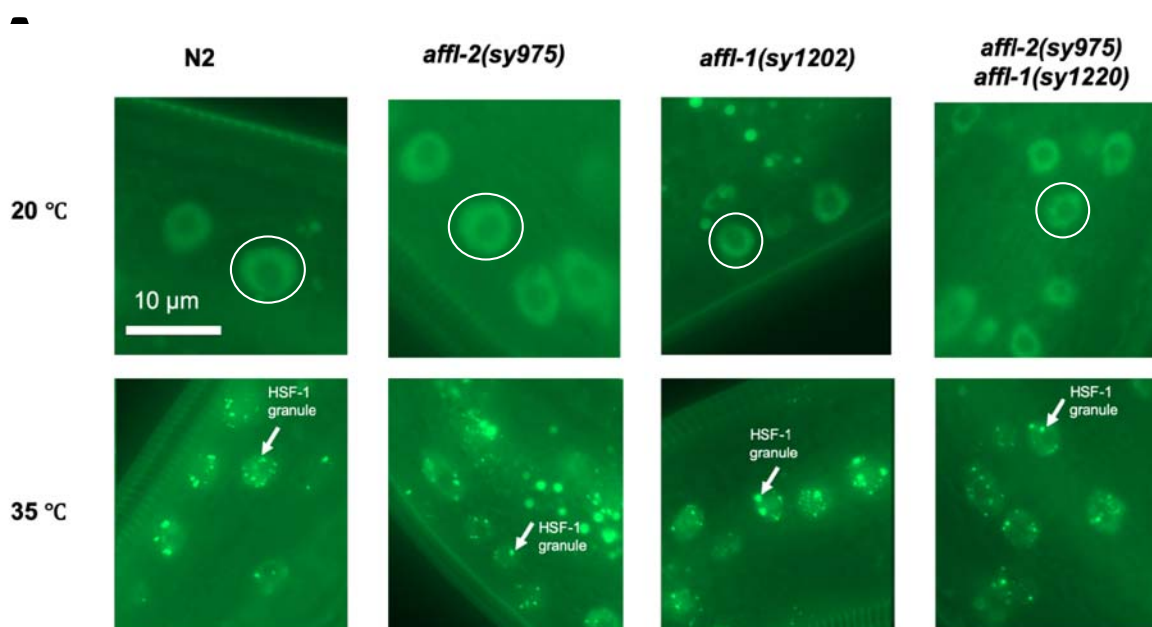
750

751



752

753 **Figure 3. AFFL-2 is a ubiquitously expressed nuclear protein.** A) Representative image of a
754 worm expressing *Paffl-2::cGAL > 15xUAS::GFP::H2B*, which can be seen in the majority of
755 cells, indicating that *affl-2* is ubiquitously expressed. Note that the effector construct is
756 integrated, while the driver is an extrachromosomal array. B) AFFL-2::GFP at 20 °C and 33 °C.
757 Both images are taken of nuclei in the tail of young adults.
758 (C) Diagrams of AFFL-2 variants. Note that diagrams are not to scale, but are just representative
759 of the ordering of various elements. FUS LC* represents the modified FUS LC residues with
760 disordered residues mutated to more ordered ones. All constructs are driven by the *affl-2*
761 promoter (*Paffl-2*). (D) Subcellular localization of AFFL-2 variants. Animals in photos are
762 young wild type adults at room temperature. (E) Fraction of worms pumping before or after heat
763 shock to induce *hsp-16.41: lin-3c* expression. Data are a proxy for gene expression (pumping
764 quiescence indicates *hsp-16.41* expression). Each point represents a different trial.
765
766



768 **Figure 4. Analysis of the interaction of *hsf-1*, *affl-2*, and *affl-1*.** All genotypes contain *drSi13*,
769 which is the single-copy transgene with *Phsf-1::HSF-1::GFP*. (A) Representative images of
770 hypodermis nuclei in young adults. Subcellular localization of HSF-1::GFP with and without a
771 five-minute heat shock at 35 °C. Prior to heat shock, HSF-1::GFP is distributed throughout the
772 nucleus for all genotypes; after heat shock HSF-1::GFP forms nuclear granules. Images of nuclei
773 are from the hypodermis but are representative of HSF-1::GFP localization throughout the entire
774 animal. In top row, representative nuclei are circled. In bottom row, examples of nuclear
775 granules are indicated with arrows. (B) Quantification of HSF-1::GFP granules per nucleus after
776 heat shock for different genotypes. Each point represents one nucleus.
777